Designing Directional Reverberators for Spatial Sound Reproduction

Benoit Alary, Archontis Politis, Stefan Bilbao

Audio Engineering Society

Conference Paper 20

Presented at the AES 5th International Conference on Audio for Virtual and Augmented Reality
2024 August 19–21, Redmond, WA, USA

Designing Directional Reverberators for Spatial Sound Reproduction

Benoit Alary[1], Archontis Politis[2], and Stefan Bilbao[3]

[1]*STMS, IRCAM, Sorbonne Université, CNRS, Ministère de la Culture Paris, France*
[2]*Audio Research Group, Computing Sciences Unit, Tampere University, Tampere, Finland*
[3]*Acoustics and Audio Group, University of Edinburgh, Room 2.10 Alison House, 12 Nicolson Square, Edinburgh, United Kingdom EH8 9DF*

Correspondence should be addressed to Benoit Alary (benoit.alary@ircam.fr)

ABSTRACT

The auralization of acoustics aims to reproduce the most salient attributes perceived during sound propagation. While different approaches produce various levels of detail, efficient methods such as low-order geometrical acoustics and artificial reverberation are often favored to minimize the computational cost of real-time immersive applications. Unlike most acoustics modeling approaches, artificial reverberators are perceptually motivated synthesis methods aiming to reproduce statistical properties occurring in a late reverberant sound field. A special class of reverberators, called directional feedback delay networks (DFDNs), produce direction-dependent reverberation perceived in anisotropic and inhomogeneous sound fields. However, due to a large parameter space, these reverberators can be complex to define, and reproducing very precise time-frequency-directional reverberation may become resource-intensive unless special care is taken in their design. This article introduces several design strategies for DFDNs used for reverberant sound field reproduction. This includes using a geometrical acoustics formulation of late reverberation to parameterize DFDNs, a perceptually-motivated reduction algorithm to limit the complexity of reproduction, a generic output grid design agnostic of the loudspeaker layouts or reproduction format, and special considerations for six-degree-of-freedom sound reproduction.

1 Introduction

The auralization of acoustics aims to reproduce the most salient attributes perceived during sound propagation [1]. Acoustics auralization often relies on simulation in order to produce a room impulse response (RIR) based on parameters such as a room's geometry and wall conditions. The image source method (IS) [2, 3] is a popular geometrical acoustics algorithm (GA), which considers a sound source reflecting successively at a room's boundaries, leading to a collection of image sources; responses from these are then added at a listener location, incorporating the direction and distance of the individual image sources.

Computing high-order reflections using the IS method is not considered efficient and several approaches have been proposed to estimate the omnidirectional reverberation characteristics of parallelepipedal rooms based on the IS method and using statistical reverberators to synthesize the energy decay [4, 5, 6, 7, 8, 9]. In the context of acoustics auralization, directional characteristics of late reverberation are important to consider in rooms that exhibit perceptually salient anisotropic decay characteristics [10]. As such, a formulation of directional reverberation based on the IS method was recently proposed [9] and considers impedance-based absorption and the direction of arrival of reflections to define anisotropic reverberation times in a parallelepipedal room.

The Feedback Delay Network (FDN) [11], is an artificial reverberator that synthesizes late reverberation from frequency-dependent reverberation times [12, 13], such as decay characteristics of a measured RIR [13, 14]. A special class of FDNs, called directional feedback delay networks (DFDNs) [15], are designed to synthesize direction-dependent reverberation perceived in anisotropic sound fields. In a DFDN, delay groups are specified using frequency-dependent decay times for a set of directions. The system may be designed to process either ambisonic channels [15] or a discrete set of incident plane waves represented on a spherical grid [16, 17].

One challenge of DFDN design is balancing the computational cost required for higher fidelity of reproduction with our ability to perceive directional reverberation [10]. Furthermore, while it can be demonstrated that late reverberation is independent of the listening position in a room [18, 9], in practice, spatially inhomogeneous reverberation may be observed in measurements of complex spaces [19] and in multiroom environments [20], and thus should be considered for reverberant sound field reproduction. In [17], directional- and position-dependent decay characteristics are analyzed from a set of position-dependent measurements, informing the parameters of a DFDN reverberator, which are then modulated to synthesize the reverberation when changing position. In [20], the reverberation times of a large set of RIR measurements distributed across two connected rooms are analyzed and reduced to a small number of prominent decays. For sound reproduction, a set of synthesized RIRs are mixed together with position and direction-dependent amplitudes to approximate the energy decay of measurements [21].

In this article, we propose the use of the IS formulation [9] to parametrize DFDNs, and a perceptually-motivated reduction algorithm minimizing the number of delay groups required in the reverberator. The following section reviews relevant background theory on DFDNs and the IS formulation, Section 3 covers the proposed reverberation time reduction algorithm, Section 4 examines frequency-dependent synthesis and DFDN design, and concluding remarks appear in Section 5.

2 Background

2.1 Directional Feedback Delay Network

Directional Feedback Delay Networks (DFDNs) [15, 16] are delay-based reverberators inheriting the properties of FDNs [11]. However, whereas multichannel FDNs may produce decorrelated channels sharing a unique frequency-dependent reverberation time envelope [13], DFDNs generalize the formalism to direction-dependent decay characteristics by embedding a spatial representation of signals in the recirculation path of the reverberator. In previous publications, generalized DFDNs were defined for higher-order ambisonics (HOA) [15], as well as directional grids, where each channel corresponds to a direction on a spatial grid [16]. In [16], the reverberator contains K output channels, implemented as delay-groups, and the system contains N delay lines per group, each of which corresponds to an independently processed FDN. With these configurations, defining an optimal output grid is essential since increasing the number of channels has a linear cost.

The main design parameters of FDNs and DFDNs are the decay rates and output magnitudes, both of which are typically realized using cascaded filters [22] for frequency-dependent control. For a direction $\mathbf{u}$ and frequency ω, we calculate the per sample attenuation of a reverberator from a specified $\mathrm{RT}_{60}(\mathbf{u},\omega)$ through

$$g_{\mathrm{dB}}(\mathbf{u},\omega) = \frac{-60}{\mathrm{RT}_{60}(\mathbf{u},\omega) f_{\mathrm{s}}}, \tag{1}$$

the resulting gains are used to specify absorption filter [22] in the recirculation path of the reverberator, as defined by

$$\mathbf{g}_i(\mathbf{u},\omega) = (10^{\frac{g_{\mathrm{dB}}(\mathbf{u},\omega)}{20}})^{\mathbf{m}_i}, \tag{2}$$

where $\mathbf{m}_i$ is the delay length vector of the ith delay group in a DFDN.

In this article, to minimize the order of the system, we consider grouping the different grid directions $\mathbf{u_i}$ into non-continuous sphere segments, each sharing similar frequency-dependent decay profiles.

2.2 Image Source Method

The image source method (IS) [2, 3], is a geometrical acoustics approach considering individual reflections as virtual sound sources originating from "mirror" rooms. For the attenuation of individual reflection paths, most GA methods rely on energy-based and random incidence sound absorption coefficients, measured in a diffuse sound field [23]. However, impedance-based absorption [24, 25], which considers the reflection angle at the surface boundaries, has been shown to improve the simulation accuracy of GA methods [26, 27, 28, 29].

Recently, a formulation of reverberation time in a parallelepipedal room was derived from the IS [9], and considers both angle-dependent absorption and directional reverberation. In the IS formula, the directional reverberation time $\mathrm{RT}_{60}(\mathbf{u})$, for a fixed direction $\mathbf{u}$, is defined as [9]

$$\mathrm{RT}_{60}(\mathbf{u}) = \frac{6\ln(10)}{\mathrm{K}(\mathbf{u})}, \tag{3}$$

where

$$\mathrm{K}(\mathbf{u}) = -c\sum_{\nu=1}^{3}\sum_{\alpha=+,-}\frac{\ln(|\beta_\nu^\alpha|)|u_\nu|}{L_\nu} \geq 0, \tag{4}$$

for a given angle-dependent reflectance defined as

$$\beta_\nu^\alpha(\mathbf{u}) = \frac{z_\nu^\alpha|u_\nu|-1}{z_\nu^\alpha|u_\nu|+1}, \tag{5}$$

where z is the surface impedance, for walls $\nu = 1,\cdots,3$ with $\alpha = +,-$. The angle-independent reflectance, is defined as

$$\beta_\nu^\alpha = \sqrt{1-a_\nu^\alpha}, \tag{6}$$

where a is an absorption coefficient. When z or a are defined over frequency bands ω, we can resolve Eq.3 as $\mathrm{RT}_{60}(\mathbf{u},\omega)$. The time-integrated energy received is defined as

$$E(\tau_\Delta,\mathbf{u}) = \frac{e^{-\mathrm{K}(\mathbf{u})\tau_\Delta}}{16\pi^2c^2\tau_\Delta^2}. \tag{7}$$

Using this formulation, a definition of the reverberation is given for angles on a sphere. The following section explores practical solutions to the design of a DFDN reverberator specified using this formulation of reverberation time.

3 Directional Decay Reduction

The DFDN and the IS formula both consider the anisotropic characteristics of late reverberation. As such, Eq.3 may be used to define directional decays in a DFDN from a specification of room dimensions and absorption coefficients. However, since the IS formula is an expression of continuously varying directional decays, we require a conversion method to obtain a smaller number of decays, used for reproduction. Here, we propose a reduction algorithm, preserving the predominant directional reverberation features from the IS formula. This approach is perceptually motivated as it will *accentuate* the coverage of some of the most predominant decay characteristics of the IS formulation. This principle carries over in Sec.4, where analysis results are simplified to a subset of frequency-dependent decay profiles.

3.1 Quantization and Segmentation

We define reverberation time for a set of D directions, $\mathbf{RT}_{60} = [\mathrm{RT}_{60}(\mathbf{u}_1),\ldots,\mathrm{RT}_{60}(\mathbf{u}_D)]$ using Eq.3. In Fig.1a, we resolve $\mathbf{RT}_{60}$ on a dense spherical t-design grid with $D = 21000$. For illustrative purposes, we use an example room with a size of 15m, 20m, and 30m, along the x, y, and z axis. The surface impedances z_ν^α are set to 10, 20, and 4 respectively, for the positive x, y, and z walls ($\alpha = +$), and 10, 7, and 10 for negative walls ($\alpha = -$).

From these parameters, we obtain 21000 unique values ranging between 0.2292 and 2.0725 seconds. We may, for instance, quantize these values by rounding to the nearest 0.01-second ($\lfloor\mathbf{RT}_{60}(\phi,\theta)\rceil_{0.01}$), yielding 21 unique values. This is significantly smaller, yet, it is unlikely that this level of detail is necessary for reproduction. As such, a statistical approach is favored for a finer and more flexible quantization, preserving a smaller set of predominant decay features.

The median cut algorithm, originally developed in the context of computer graphics [30], is an iterative algorithm used to quantize the colors of an image to a fixed set of Q unique colors. Starting from a list of values,

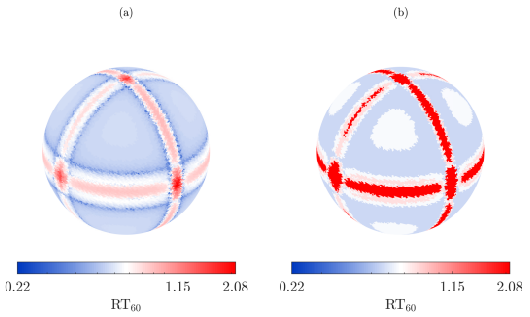

Fig. 1: *(a)* $\mathbf{RT}_{60}$ *values from the IS formula, and (b)* $\mathbf{RT'}_{60}$ *quantized to* $Q = 4$ *values (0.56, 0.65, 0.77, 2.07).*

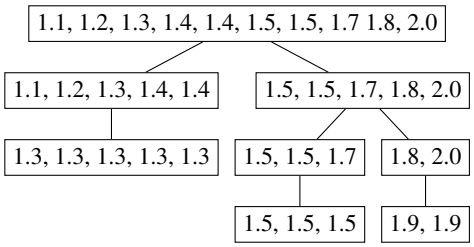

Fig. 2: *Example result from the median cut algorithm on a list of values with* $Q = 3$*. The last row contains the median of each sublists.*

the first step consists of splitting the list into two segmented lists, containing the values that are either $\leq$, or $>$ its median value. In the following steps, we choose the list with the widest range of values and dividing it at its median value (Fig.2), and repeat this procedure until we reach a chosen amount of Q lists. Here, Q is chosen with respect to a computational budget for a given application.

The final step consists of replacing the values of each segmented list with either its mean, median, mode, or maximum value. This brings the number of unique values to Q. In the context of reverberation time on a grid, the median cut algorithm will yield a non-continuous segmentation of the directional grid, grouping the directions sharing a smaller range of values. Here, we quantize each segmented list using their respective maximum value to obtain a final quantized list $\mathbf{RT'}_{60}$, as illustrated in Fig.1b.

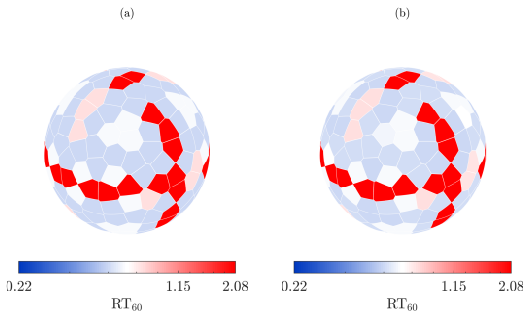

Fig. 3: *(a) Quantized and sampled values from Fig.1b, and (b) the analysis results of a realization of these decay parameters in a DFDN.*

3.2 Grid Reduction

While the median cut segmentation reduces the number of unique RT_{60} values, a smaller spatial grid is necessary for sound reproduction. We thus convert the dense grid $\mathbf{U}_{\text{grid}} = [\mathbf{u}_1, ..., \mathbf{u}_D]$ to a sparse grid $\mathbf{U'}_{\text{grid}} = [\mathbf{u'}_1, ..., \mathbf{u'}_K]$ with $K << D$. The points of the dense grid are clustered into K clusters according to their angular distance to the sparse grid points, as indicated by a clustering variable p_d assigning the dth point on the high-resolution grid to the kth point on the sparse grid

$$p_d = \arg\min_k \arccos(\mathbf{u}_d \cdot \mathbf{u}'_k). \tag{8}$$

We denote the set of indices of points $\mathbf{u}_d$ assigned to point $\mathbf{u}_k$ as $\mathcal{A}_k = \{d | p_d = k\}$. The high resolution reverberation times after quantization assigned to the kth point are then denoted as $\mathbf{RT'}_{60}^{(k)} = \{RT'_{60}(\mathbf{u}_i) | i \in \mathcal{A}_k\}$. The final $RT_{60}^{(k)}$ value assigned to point $\mathbf{u}'_k$ is then resolved as the mode of the respective list of clustered reverberation times, i.e. $RT_{60}^{(k)} = \text{Mode}(\mathbf{RT'}_{60}^{(k)})$. The final reduced list of quantized values on the K-point grid is denoted as $\widetilde{\mathbf{RT'}}_{60}^{K}$.

The results of this process, for a uniform t-design grid with $K = 216$, are as illustrated in Fig.3a. From this, we now have a reduced set of RT_{60} values that we can use to specify a DFDN. In turn, the output signals of a DFDN realized through these parameters, is

re-analyzed to validate that the target reverberation times are produced by the system as expected (Fig.3b). The implementation details of this DFDN, along with frequency-dependent considerations, are specified in the next section.

4 Frequency-Dependent Synthesis

In the previous section, we reduced a set of directional $\mathbf{RT}_{60}$ obtained using the image source formula (Eq.3) to a quantized set of values $\mathbf{RT}'_{60}$ on a smaller grid $\widetilde{\mathbf{RT}'}^{K}_{60}$. This formulation can also be realized using a set of frequency-dependent absorption coefficients. In this section, we demonstrate how frequency-dependent decay characteristics ($\mathbf{RT}_{60}(\omega)$) are used to specify a DFDN with a fixed order.

As reference data, we use a measured spatial room impulse response (SRIR) (seat 280, row 8, center stage sound source in the OperaRIR dataset [19][1]). A reverberation time analysis is performed on direction-, time-, and frequency-dependent energy decay functions [31], and the individual $\mathbf{RT}_{60}(\omega)$ are characterized using a segment of the decaying slopes, between a mixing time and a noise floor time [32] (Fig.7). The slope analysis also provides the initial directional power spectrum $\mathbf{P}_0(\omega)$ [32], corresponding to the magnitude of the estimated slopes at time 0. In this section, we will use the decay analysis results from a K-point directional grid and quantize them to Q decay profiles, in turn, used to define a segmented DFDN reverberator to produce K output signals.

4.1 Frequency-Dependent Quantization

The median cut algorithm (Sec.3.1) was originally developed to quantize colors on red/green/blue axes [30]. As such, using the same principle, we may use data with multiple frequency-axes. At each step, we search for the list containing the band ω with the widest range of $\mathrm{RT}_{60}(\omega)$ values and divide this list between the directions where the values of the chosen band is below or above its median. Once we have obtained Q segmented lists, we quantize the values of each band contained in each list to either its respective mean, median, mode, or maximum value, for a final quantized list $\mathbf{RT}'_{60}(\omega)$. As such, each direction within a segment shares the same frequency-dependent profile (Fig.4).

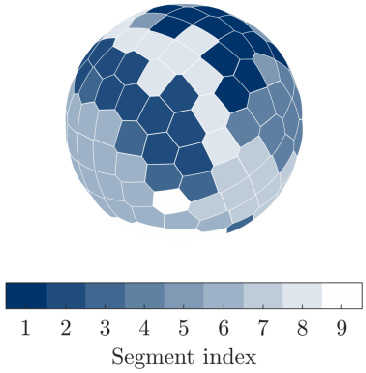

Fig. 4: *Non-continuous sphere segmentation after the median cut algorithm ($Q = 9$)*

4.2 Segmented DFDN

In a generalized DFDN, internal delay groups correspond to a sub-reverberator assigned to a specific output channel [15, 16]. Since each sub-reverberator is can produce several decorrelated channels, we propose to reduce the number of delay groups to Q, the amount of unique directional decay profiles contained in $\mathbf{RT}'_{60}(\omega)$, thus minimizing the internal processing of the reverberator (Fig.5). The output $\mathbf{y}$ of the modified DFDN is defined as

$$\mathbf{y}(z) = \mathbf{C}(z)\mathbf{M}\mathbf{s}(z) \tag{9a}$$

$$\mathbf{s}(z) = \mathbf{G}(z)\mathbf{Z}(z)\Big[\mathbf{b}\odot\mathbf{x}(z)+\boldsymbol{\mathcal{A}}\mathbf{s}(z)\Big], \tag{9b}$$

where $\odot$ denotes an element-wise multiplication (Hadamard product), and $\mathbf{s}(z)$ corresponds to a concatenated vector

$$\mathbf{s}(z) = [s_{1,1}(z),...s_{1,Q}(z),s_{2,1}(z),...,s_{N,Q}(z)]^T, \tag{10}$$

and $\mathbf{b}$ is the input gain vector of length $Q\cdot N$, defined as

$$\mathbf{b} = [\mathbf{b}_1^T,...,\mathbf{b}_N^T]^T, \tag{11}$$

and $\mathbf{Z}$ is a diagonal matrix of delay lines. The recirculating gain matrix is defined as $\boldsymbol{\mathcal{A}} = \mathbf{A}\otimes\mathbf{I}_Q$, where $\mathbf{A}$ is an unitary matrix of size $N\times N$, $\otimes$ is the Kronecker product, and $\mathbf{I}_Q$ is the identity matrix of size $Q\times Q$

[1] https://doi.org/10.5281/zenodo.8096639

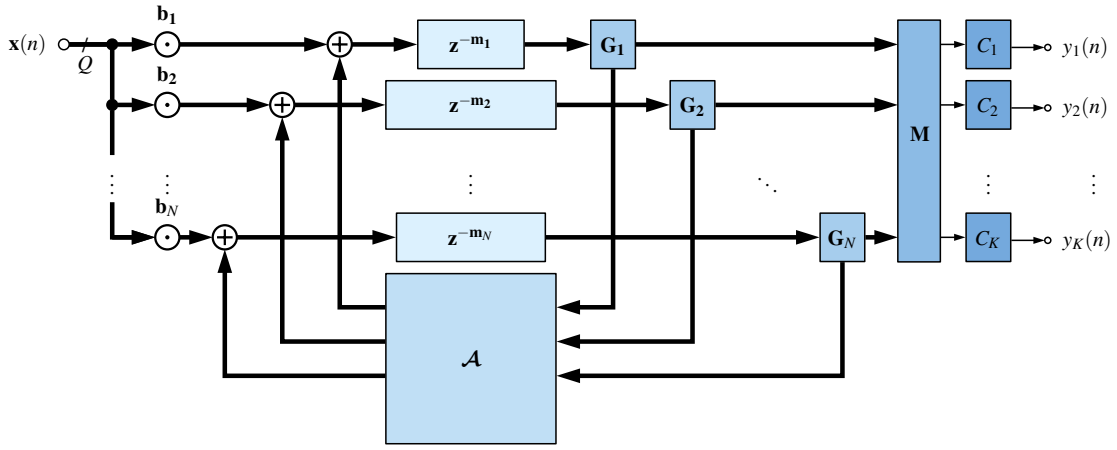

Fig. 5: *Flow diagram of the segmented DFDN.*

[16]. The diagonal matrix **G** contains the absorption filters, ensuring energy decay in the system. The multichannel input signal **x** typically contains Q copies of a mono input signal, but may also contain spatially distributed signals, such as early reflections, if the input channel ordering is coherent with the output stages of the reverberator $(\mathbf{M}, \mathbf{C}, \mathbf{y})$.

In the segmented DFDN, **M** is a mixing matrix of size $K \times Q \cdot N$, containing the mixing gains for the K final output channels. Typically, **M** is a binary matrix mapping one of the $Q \cdot N$ signals to one of the K output channels, but this matrix may also be used to produce more decorrelated outputs for low orders of N by combining multiple recirculating outputs [33]. Similarly to the generalized DFDN [15], tone-correction filters C are placed before the output channels to adjust the gains and spectral coloration of the output signals.

The absorption filters **G** and the tone-correction filters **C**, are realized through a series of cascaded peak-notch filters distributed on octave bands [22]. The gains of the absorption filters are calculated using Eq.1-2 with $\mathbf{RT}'_{60}(\omega)$. The tone-correction filters $\mathbf{C}(z)$ are designed from a directional power spectrum $\mathbf{P}_0(\omega)$, either using (Eq.7), or from analysis results [12]. Note that the $\mathbf{P}_0(\omega)$ values are not quantized since the **C** reside outside the recirculation paths of the reverberator.

This approach, based on graphical equalization filters (GEQ), may suffer from the interaction between the various octave-band filters, leading to a loss of precision between the target gain values, known as command

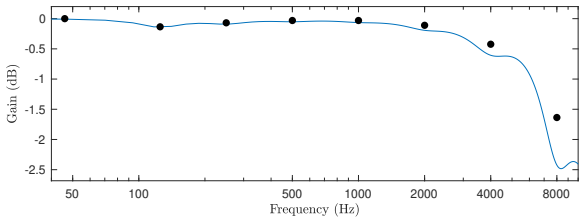

Fig. 6: *Example response from one of the cascaded attenuation filters (G_i) in the DFDN. The black dots represent the command gains of the multiband EQ.*

gains, and the frequency-response of the cascaded filter (Fig.6). For a more accurate frequency-dependent reproduction, several approaches may be considered [34, 35, 36, 37].

At this stage, we have K reverberant signals on a system-agnostic spherical grid. The final step is to pan or encode these signals to a specific final output channel configuration (hemispherical loudspeaker setup, binaural, ambisonics, a.o.). For loudspeaker systems, one approach is to use vector-base amplitude panning [38, 16]. However, to ensure the decorrelation of late reverberation signals on multiple loudspeakers, a simpler approach is to mix all the signals to their closest loudspeaker (see Eq.8), assuming fewer loudspeakers than the K grid points.

The final results, analyzed from a DFDN specified from $\mathbf{RT}'_{60}(\omega)$ and $\mathbf{P}_0(\omega)$ parameters is illustrated in Fig.8. We observe that the main spatial characteristics of the

250Hz band, which has the longest reverberation time and widest range of decay values, are well preserved, while some loss of spatial characteristics occurs at other bands. We also observe that the range of frequency-dependent values, at 2kHz for instance, seemingly suffers from the rudimentary filter design Fig.6. This loss of both spatial and frequency decay accuracy is deemed acceptable and part of the required compromise made for optimal real-time synthesis.

4.3 Six Degrees of Freedom

For 6DoF reproduction, as detailed in [17], the gains in the absorption and tone-correction filters are modulated over a short period to modify the directional decay according to reference configurations. New configurations may be obtained for any point in space by averaging over several data points [17].

With a segmented DFDN, when the sphere segmentation is modified, it is preferable to assign the decay of the segmented delay groups in a consistent order of decay length, to ensure a smoother cross-fade between directional decay distribution, such as ordering each Q segment based on decreasing value of reverberation time of a reference band (ω_{ref}). Furthermore, the gains in the output mixing matrix $\mathbf{M}$ should also be cross-faded over several frames to ensure smooth modulation when changing the segment-to-output configuration. One benefit of using a delay network for 6DoF reproduction, it that the system has a fixed cost and the quantized $\mathbf{RT}'(\omega)$ values and grid segmentation can vary at each location. As such, this method supports the reproduction of inhomogeneous rooms [19].

5 Conclusion

In this work, we have demonstrated how a formulation of decay times in the IS method or slope analysis results from measurements may be used, quantized, and reduced to a small subset of unique frequency-dependent decay profiles. Using this simplified representation of reverberation around a listening sphere, a segmented DFDN reverberator may be specified to produce artificial reverberation. The level of detail is controlled by a single parameter determining the number of non-continuous segments on a sphere, and the segmentation is performed using a perceptually motivated algorithm reducing a set of frequency-dependent decay times based on the range of values.

Overall, due to the ability of DFDNs to produce multiple decorrelated signals, this framework offers more flexibility than other convolution-based simplification methods used for the auralization of large sets of varying decay rates. Future work will include improving the frequency-domain accuracy of reproduction and subjective evaluation to demonstrate the benefits of this method in preserving the most salient characteristics of late reverberation in the context of 6DoF sound reproduction.

6 Acknowledgement

The work of the first author is related to the activities of the Continuum project supported by the Cultural and Creative Industries area of the France 2030 initiative.

References

[1] Vorländer, M., *Auralization*, Springer-Verlag, Berlin, 2008.

[2] Eyring, C. F., "Reverberation Time in "Dead" Rooms," *The Journal of the Acoustical Society of America*, 1(168), pp. 168–168, 1930.

[3] Allen, J. and Berkley, D., "Image method for efficiently simulating small-room acoustics," *J. Acoust. Soc. Am.*, 65(4), pp. 943–950, 1979.

[4] Lehmann, E. and Johansson, A., "Prediction of energy decay in room impulse responses simulated with an image-source model," *J. Acoust. Soc. Am.*, 124(1), pp. 269–277, 2008.

[5] Lehmann, E. A. and Johansson, A. M., "Diffuse Reverberation Model for Efficient Image-Source Simulation of Room Impulse Responses," *IEEE Trans. Audio, Speech, Language Proces.*, 18(6), pp. 1429–1439, 2010.

[6] Accolti, E. and Miyara, F., "Fast and controllable box-shaped room impulse response algorithm," *XIII Reunión de Trabajo en Procesamiento de la Información y Control, RPIC*, 2009.

[7] Nogueiras Rodríguez, A. and Colom Olivares, J., "A statistical approach to reverberation in non-diffusive rectangular rooms based on the image source model," in *IEEE Int. Conf. Acoust., Speech Sig. Proces.*, pp. 448–452, 2013.

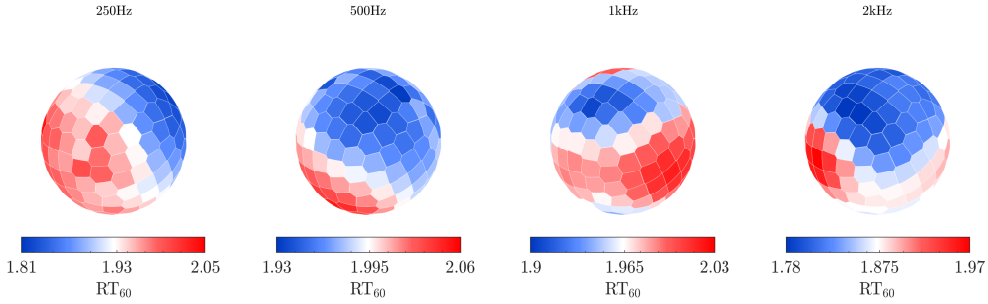

Fig. 7: *Reference directional reverberation analysis from a measured SRIR [19].*

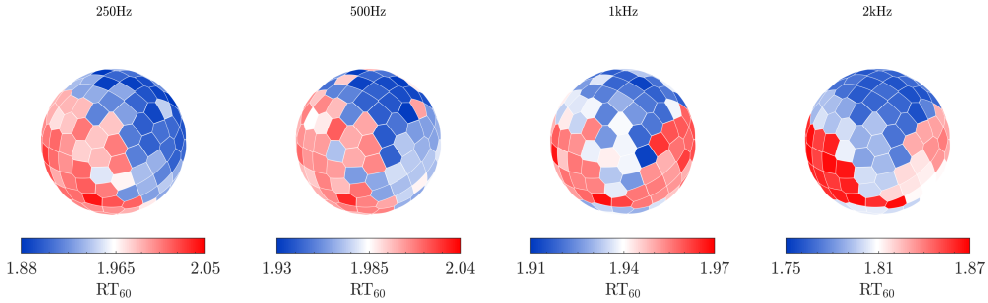

Fig. 8: $\mathbf{RT}_{60}$ *analysis results from the output of a DFDN specified from the reduced* $\mathbf{RT}'_{60}$ *values* ($Q = 9$).

[8] Schlecht, S. J., Prawda, K., Rabenstein, R., and Schäfer, M., "Damping Density of an Absorptive Shoebox Room Derived from the Image-Source Method," *Arxiv*, 2023.

[9] Bilbao, S. and Alary, B., "Directional reverberation time and the image source method for rectangular parallelepipedal rooms," *The Journal of the Acoustical Society of America*, 155(2), pp. 1343–1352, 2024.

[10] Alary, B., Massé, P., Schlecht, S. J., Noisternig, M., and Välimäki, V., "Perceptual Analysis of Directional Late Reverberation," *J. Acoust. Soc. Am.*, 149(5), pp. 3189–3199, 2021.

[11] Jot, J.-M. and Chaigne, A., "Digital Delay Networks for Designing Artificial Reverberators," in *Proc. Audio Eng. Soc. 90th Conv.*, Paris, France, 1991.

[12] Jot, J.-M., "An analysis/synthesis approach to real-time artificial reverberation," in *Proc. IEEE ICASSP-92*, volume 2, pp. 221–224, San Francisco, CA, 1992.

[13] Jot, J.-M., Cerveau, L., and Warusfel, O., "Analysis and Synthesis of Room Reverberation Based on a Statistical Time-Frequency Model," in *Proc. Audio Eng. Soc. 103rd Conv.*, New York, USA, 1997.

[14] Dal Santo, G., Alary, B., Prawda, K., Schlecht, S. J., and Välimäki, V., "RIR2FDN: An Improved room impulse response analysis and synthesis," in *Proc. DAFx*, 2024.

[15] Alary, B., Politis, A., Schlecht, S., and Välimäki, V., "Directional Feedback Delay Network," *J. Audio Eng. Soc.*, 67(10), pp. 752–762, 2019.

[16] Alary, B. and Politis, A., "Frequency-Dependent Directional Feedback Delay Network," in *Proc. IEEE ICASSP-2020*, pp. 176–180, 2020.

[17] Alary, B. and Välimäki, V., "A Method for Capturing and Reproducing Directional Reverberation in Six Degrees of Freedom," in *Proc. Int. Conf. Immersive and 3D Audio*, Bologna, Italy, 2021.

[18] Kuttruff, H., *Room Acoustics, Fifth Edition*, Taylor & Francis, 2009.

[19] Alary, B. and Politis, A., "A Dataset for Location- and Direction-Dependent Reverberation Analysis," in *10th Convention of the European Acoustics Association Forum Acusticum 2023*, pp. 1663–1670, Turin, Italy, 2023.

[20] Götz, G., Schlecht, S. J., and Pulkki, V., "Common-Slope Modeling of Late Reverberation," *IEEE/ACM Transactions on Audio, Speech, and Language Processing*, 31, pp. 3945–3957, 2023.

[21] Götz, G., Kerimovs, T., Schlecht, S. J., and Pulkki, V., "Dynamic late reverberation rendering using the commonslope model," in *Proc. Audio Eng. Soc. 6th Int. Conf. on Audio for Games*, Tokyo, Japan, 2024.

[22] Välimäki, V. and Reiss, J. D., "All about audio equalization: Solutions and Frontiers," *Appl. Sci.*, 6(5), 2016.

[23] Sabine, W., *Collected Papers on Acoustics*, Harvard University Press, Cambridge, MA, USA, 1922.

[24] Hunt, F., Beranek, L., and Maa, D., "Analysis of Sound Decay in Rectangular Rooms," *J. Acoust. Soc. Am.*, 11(1), pp. 80–94, 1939.

[25] Wenzel, A., "Propagation of waves along an impedance boundary," *J. Acoust. Soc. Am.*, 55(5), pp. 956–963, 1974.

[26] Jeong, C.-H. and Rindel, J., "A Study on the Characteristics of Phased Beam Tracing Method for the Acoustic Simulation of an Enclosure at Mid Frequencies," in *Proc. WESPAC IX 2006, The 9th Western Pacific Acoustics Conference*, 2006.

[27] Aretz, M., Dietrich, P., and Vorländer, M., "Application of the Mirror Source Method for Low Frequency Sound Prediction in Rectangular Rooms," *Acta Acustica u. Acustica*, 100(2), pp. 306–319, 2014.

[28] Marbjerg, G., Brunskog, J., Jeong, C.-H., and Nilsson, E., "Development and validation of a combined phased acoustical radiosity and image source model for predicting sound fields in rooms," *J. Acoust. Soc. Am.*, 138(3), pp. 1457–1468, 2015.

[29] Mondet, B., Brunskog, J., Jeong, C.-H., and Rindel, J., "From absorption to impedance: Enhancing boundary conditions in room acoustic simulations," *Appl. Acoust.*, 157, p. 106884, 2020.

[30] Heckbert, P., "Color image quantization for frame buffer display," *ACM Siggraph Computer Graphics*, 16(3), pp. 297–307, 1982.

[31] Schroeder, M. R., "New Method of Measuring Reverberation Time," *J. Acoust. Soc. Am.*, 37(3), pp. 409–412, 1965, doi:10.1121/1.1909343.

[32] Massé, P., Carpentier, T., Warusfel, O., and Noisternig, M., "Denoising Directional Room Impulse Responses with Spatially Anisotropic Late Reverberation Tails," *Applied Sciences*, 10(3), 2020.

[33] Schroeder, M. R. and Logan, B. F., "'Colorless' Artificial Reverberation," *J. Audio Eng. Soc.*, 9(3), pp. 192–197, 1961.

[34] Jot, J.-M., "Proportional parametric equalizers—Application to digital reverberation and environmental audio processing," in *Proc. 139th AES Conv.*, 2015.

[35] Liski, J. and Välimäki, V., "The quest for the best graphic equalizer," in *Proc. DAFx*, pp. 95–102, 2017.

[36] Prawda, K., Schlecht, S. J., and Välimäki, V., "Improved Reverberation Time Control for Feedback Delay Networks," in *Proc. DAFx*, pp. 299–306, 2019.

[37] Välimäki, V., Prawda, K., and Schlecht, S. J., "Two-Stage Attenuation Filter for Artificial Reverberation," *IEEE Signal Process. Lett.*, 31, pp. 391–395, 2024.

[38] Pulkki, V., "Virtual Sound Source Positioning Using Vector Base Amplitude Panning," *J. Audio Eng. Soc.*, 45(6), pp. 456–466, 1997.